HHS Public Access

Author manuscript

Cancer Immunol Res. Author manuscript; available in PMC 2020 March 01.

Published in final edited form as:

Cancer Immunol Res. 2019 March ; 7(3): 510–525. doi:10.1158/2326-6066.CIR-18-0054.

Immune-Checkpoint Blockade Opposes CD8+ T-cell Suppression in Human and Murine Cancer

Lukas W. Pfannenstiel[1], **C. Marcela Diaz-Montero**[1], **Ye F. Tian**[1], **Joseph Scharpf**[2,4], **Jennifer S. Ko**[3], and **Brian R. Gastman**[1,4,5]

[1]Department of Immunology, Lerner Research Institute

[2]Department of Otolaryngology

[3]Departments of Pathology and Dermatology

[4]Institutes of Head and Neck, Dermatology and Plastic Surgery

[5]Taussig Cancer Center, Cleveland Clinic, Cleveland, OH, USA

Abstract

Immune-checkpoint blockade enhances antitumor responses against cancers. One cancer type that is sensitive to checkpoint blockade is squamous cell carcinoma of the head and neck (SCCHN), which we use here to study limitations of this treatment modality. We observed that $CD8^+$ tumor infiltrating lymphocytes (TIL) in SCCHN and melanoma express excess immune checkpoints components PD-1 and Tim-3 and are also $CD27^-/CD28^-$, a phenotype we previously associated with immune dysfunction and suppression. In *ex vivo* experiments, patients' $CD8^+$ TILs with this phenotype suppressed proliferation of autologous peripheral blood T cells. Similar phenotype and function of TILs was observed in the TC-1 mouse tumor model. Treatment of TC-1 tumors with anti-PD-1 or anti-Tim-3 slowed tumor growth in vivo and reversed the suppressive function of multi-checkpoint$^+$ $CD8^+$ TIL. Similarly, treatment of both human and mouse PD-1^+ Tim-3^+ $CD8^+$ TILs with anti-checkpoint antibodies *ex vivo* reversed their suppressive function. These suppressive $CD8^+$ TILs from mice and humans expressed ligands for PD-1 and Tim-3 and exerted their suppressive function via IL10 and close contact. To model therapeutic strategies, we combined anti-PD-1 blockade with IL7 cytokine therapy or with transfer of antigen specific T cells. Both strategies resulted in synergistic antitumor effects and reduced suppressor cell function. These findings enhance our understanding of checkpoint blockade in cancer treatment and identify strategies to promote synergistic activities in the context of other immunotherapies.

Introduction

Tumor-infiltrating $CD8^+$ T cells in human and mouse cancers express excess checkpoint inhibitor proteins, signaling molecules that inhibit T-cell function and negatively regulate normal T-cell responses (1,2). In mice, blocking checkpoint proteins, such as programmed

Corresponding Author: Brian R. Gastman, M.D., Cleveland Clinic Lerner Research Institute, Department of Immunology, 9500 Euclid Ave, NE60, NE6-303, Ph. 216-445-2103, Fax. 216-445-4658, gastmab@ccf.org.

Conflict of Interest Statement: The authors declare that no conflict of interest exists.

death receptor 1 (PD-1) and T-cell immunoglobulin and mucin protein 3 (Tim-3), enhances antitumor $CD8^+$ T-cell responses and slows tumor growth(3,4). With the increased application of combination strategies for cancer therapy (over 800 current clinical trials include some form of PD-1 inhibitor), a more complete understanding of the biology of checkpoint inhibitors is critical (5).

Squamous cell carcinoma of the head and neck (SCCHN) is one of the deadliest human cancers, with few treatment options once a patient has failed conventional therapies(6). The rise of HPV^+ variants has led to an increased incidence of SCCHN among younger and non-smoking patients (7). As metastatic SCCHN of both types continues to present a treatment challenge, there is increased interest in the use of immunotherapies to augment existing treatments (8,9). Although anti-PD-1 therapies have are FDA approved for SCCHN, their effects are modest compared to those in melanoma and other cancers (10,11). Thus, SCCHN is a challenging setting in which to develop a broadly applicable immunotherapy.

We and others observed that SCCHN tumor cells can convert normal $CD8^+$ T cells from cytotoxic effectors to inhibitors of antitumor immunity (12–14). We showed that cell lines derived from SCCHN induce $CD8^+$ T cells to become suppressor cells and lose expression of CD27 and CD28 (12). We found that the loss of CD27 and CD28 expression was a common occurrence in SCCHN patients' peripheral blood lymphocytes (13). We abrogated the tumor induced T-cell changes by treatment of tumor-exposed T cells with interleukin-7 (IL7) cytokine (13).

Here, we demonstrate that loss of CD27 and CD28 expression in patient derived $CD8^+$ TILs from both HPV^+ and HPV^- SCCHN (as well as melanoma) is accompanied by de novo expression of multiple checkpoint proteins, particularly PD-1 and Tim-3. We show that $CD8^+$ T cells isolated from a murine HPV-E6 and E7 expressing squamous cell carcinoma (SCC) have a similar phenotype. Unexpanded and untreated human and mouse $PD\text{-}1^+$ $Tim\text{-}3^+$ $CD8^+$ T cells obtained from tumors suppressed the proliferative capacity of normal autologous T cells. Antibody blockade of PD-1 and Tim-3 slowed tumor growth in association with enhanced $CD8^+$ T-cell proliferation and function. Despite continued expression of immune checkpoint proteins, the suppressive activities of the tumor associated $CD8^+$ cells are abrogated following treatment with anti-checkpoint antibodies. When checkpoint-inhibitor treatment was combined with IL7 cytokine therapy or adoptive transfer of E7-specific $CD8^+$ T cells, we observed synergistic antitumor effects. This synergy was associated with reduced $PD\text{-}1^+$ $Tim\text{-}3^+$ $CD8^+$ T-cell suppressor activity. In a model of adoptive T-cell therapy, we show that without checkpoint inhibition, transferred cells themselves become suppressive. We demonstrate that blockade of PD-1 can prevent suppression by $PD\text{-}1^+$ $Tim\text{-}3^+$ $CD8^+$ T cells isolated from mouse and human tumor tissues. Mouse and human suppressive $CD8^+$ T cells express the ligands for PD-1 and Tim-3 and mediate suppression through a mechanism that requires IL10 and close contact. Thus, in addition to augmenting T-cell antitumor effector function, checkpoint inhibitors also block the generation of $CD8^+$ suppressive cells that are otherwise enriched in the tumor microenvironment.

Materials and Methods

Mice:

Six to 8-week old C57BL6 mice were purchased from the National Cancer Institute (Frederick, MD). HPV-E7 TCRβ transgenic mice have been described previously and were obtained from the laboratory of Graham R. Leggatt (University of Queensland, St. Lucia, Australia)(15). HPV-E7 TCRβ Thy1.1 mice were generated by breeding HPV-E7 TCRβ mice with C57BL/6 CD90.1 congenic mice (strain B6.PL-*Thy1*^{a}/CyJ, Stock #000406) (Jackson Laboratories) and then crossing the resulting progeny until all mice were homozygous for Thy1.1 and hemizygous for the HPV-E7 TCRβ transgene. Expression of the congenic marker was verified by flow cytometric staining of blood lymphocytes using anti-CD90.1 and anti-CD90.2 antibodies. Presence of the TCRβ transgene was verified by PCR using the following primers: Forward-5'ATCTGCAGATCAGTGCTCATCCCACTATG; Reverse-5'ATCCGCGGCCACTCTGCTAAGGTT TTCTG and by flow cytometry for TCR vβ12. PCR reaction conditions have been described previously (15). All animals were housed in the Biological Resources Unit of the Cleveland Clinic Lerner Research Institute under protocols approved by the institutional animal care and use committee in accordance with NIH Office of Laboratory Animal Welfare guidelines.

Cell Lines:

The murine TC-1 tumor cell line has been previously described (16) and was a generous gift from Dr. T.C. Wu (Johns Hopkins University) and was obtained circa 2012 and cultures derived from early aliquots were passaged no more than three times prior to use. While cells were not authenticated in the past year, mycoplasma contamination was routinely tested using the MycoAlert™ kit according to the manufacturer's protocol (Lonza, Basel, Switzerland). Cells were maintained in RPMI with 10% Fetal Bovine Serum, 10 mmol/L HEPES, 1 mmol/L sodium pyruvate, 2 mmol/L nonessential amino acids and 100u/ml penicillin/streptomycin in an incubator containing 10% CO_2.

Antibodies, flow cytometry, and cell sorting:

Fluorescently conjugated, anti-mouse antibodies were purchased from Biolegend (San Diego, CA) (CD3-PerCP, CD8 FITC, CD8 APC, PD-1 FITC, Tim-3 PE, Lag3 APC, CD90.1 PerCP, PD-L1 PerCP, Galectin-9 FITC). Fluorescently conjugated, anti-human antibodies were purchased from Biolegend (CD3-PerCP, CD8 APCcy7, CD4 PEcy7, Tim3 Brilliant Violet 421, Tim-3 PE, PD-L1 PerCP, Galectin-9 FITC) or from eBioscience (PD-1 PE, eFluor710). Prior to staining, all cells were treated with anti-FcγIII/CD16 from Biolegend according to the manufacturer's recommended protocol (human/mouse TrueStain FCX). Antibody staining was performed in phosphate-buffered saline with 0.1% fetal bovine serum or bovine serum albumin. Data were collected on FACS Calibur or LSR II instruments and analyzed with the FlowJo data analysis software (FlowJo Inc, Salem OR). Anti-PD-1 used *in vivo* was purified from hybridoma supernatant (clone G4, hamster IgG) which was a kind gift from Dr. Lieping Chen (Yale University) and has been previously demonstrated to inhibit PD-1 *in vivo*(17). Anti-Tim-3 was a generous gift of Costim Pharmaceuticals, Inc (clone 5D12, mouse IgG1) and is specific for all isoforms of mouse Tim-3 and has been

demonstrated to inhibit Tim-3 signaling *in vivo*(18). For blockade of human PD-1 and Tim-3, we used Nivolumab anti-PD-1 (Bristol-Meyers Squibb) and anti-Tim-3 clone F38–2E2 (Biolegend). Anti-cytokine antibodies used *in vivo* (anti-IL10, anti-IL6, and anti-TGFβ) for both mouse and human were purchased from R&D systems. For experiments utilizing sorted cells, labeled cells were sorted by the Cleveland Clinic Flow Cytometry Core using a FACS Aria II sorter into chilled-media containing tubes in a laminar flow hood. Ungated plots of sorted cells for each figure appear in Supplementary Fig. S1.

Patient PBL and Tumor Samples:

Matched peripheral blood lymphocytes (PBLs) and tumor specimens were obtained from patients with melanoma or head and neck squamous cell carcinoma. PBLs were obtained by venipuncture and isolated by centrifugation over a Ficoll-Hypaque gradient (GE Healthcare) and cryopreserved until further analysis or use. After surgical resection, tumor specimens were rinsed with antibiotic-containing media and minced with crossed scalpels under sterile conditions. Enzymatic digestion was then used to dissociate tumor tissue using 1500 u/ml collagenase IV (Gibco/Life Technologies), 1000 u/ml hyaluronidase (Sigma), and 0.05 mu/ml DNAse IV (Calbiochem) in RPMI for several hours at 37°C followed by mechanical agitation. The resulting single-cell suspensions were separated from debris by centrifugation over a Ficoll-Hypaque gradient followed by cryopreservation until further analysis.

Mouse tumor implantation, T-cell adoptive transfer, and TIL isolation:

For tumor growth experiments, 150,000 TC-1 tumor cells were implanted subcutaneously in 100 μl sterile saline and tumor growth was monitored by measuring tumor diameter with calipers every third day for the duration of the experiment. For IL7 treatment studies, 7 μg/dose of rhIL7 was injected i.p. every 24 hours for seven days starting on day 7 after tumor implantation. For antibody treatment, anti-PD-1 and/or anti-Tim-3 were injected at 100μg/dose i.p. starting seven days after tumor implantation and continuing every third day for the duration of the experiment. Studies were concluded when control-group tumor growth exceeded veterinary end-points, typically 20–30 days after implantation, and all mice were sacrificed for analysis. Tumor-infiltrating lymphocytes were isolated by disruption of tumor tissue first by mincing with crossed scalpels under sterile conditions followed by enzymatic digestion as described above. Live cells were isolated from debris by centrifugation over a Ficoll gradient prior to staining for flow cytometry or cryopreservation for further analysis. $CD8^+$ T lymphocytes were purified from tumor digests first by positive magnetic-bead isolation using anti-CD8a magnetic beads (Miltenyi Biotec) followed by cell sorting on a FACS Aria II cell sorter by the Cleveland Clinic flow cytometry core. Cells were collected into culture media and used immediately in suppression or functional assays.

In vitro suppression and function assays:

In vitro suppression assays were performed per previously-described conditions. U-bottom or V-bottom plates were coated with human or mouse anti-CD3 and anti-CD28 (10μg/ml and 5μg/ml in phosphate-buffered saline [PBS], respectively) for 3–5 hours at 37°C followed by washing out unbound antibody with PBS. Responder T cells were bulk $CD3^+$ T cells isolated from human patient PBMC or mouse splenocytes by negative magnetic bead selection using the species-appropriate kit per manufacturer's protocol (Miltenyi Biotec).

Each well contained 5×10^4 to 1×10^5 responder T cells and equal or fewer numbers of the appropriate suppressor $CD8^+$ cell population. At least three replicate wells were set up per experimental group per experiment. To measure proliferation, 72 hours after incubation, 1 μCi of ^{3}H-labeled thymidine (GE Healthcare) was added per well and incubated for a further 18–20 hours. Cells were then harvested onto filters and remaining radioactivity was measured with a Microbeta Trilux counter (Perkin-Elmer). For experiments where CFSE dilution was used as a readout, responders were labeled with 0.05–0.1 μM carboxyfluorescein succinimidyl ester (CFSE) (CellTrace kit, Life Technologies) per the manufacturer's protocol. Proliferation was measured by signal dilution on a flow cytometer. For BrdU incorporation, cells were pulsed with 10 μM BrdU for the final 24 hours of culture. Permeabilization, DNAse treatment, and staining was accomplished using the eBioscience BrdU staining kit for flow cytometry according to the manufacturer's protocol. For transwell assays, 96-well transwell plates (Milipore) with 0.4 μM pore sizes were used to separate sorted suppressor cells from responders. To assess function of sorted TIL populations (between 5×10^4 and 1×10^5 cells per well), cells were stimulated with either plate-bound CD3/CD28 (coated at 10 μg/ml and 5 μg/ml respectively) or irradiated TC-1 tumor cells (at a 1:1 ratio) for 12 hours in the presence of GolgiStop™ (BD Pharmingen) using the recommended conditions followed by intracellular cytokine staining using the cell fixation/permeablilization kit (BD Biosciences) and staining with anti-interferon γ antibody (eBioscience) and readout on a flow cytometer.

Study approval:

All human tissue was obtained at the Cleveland Clinic under a protocol approved by the institutional review board with written informed consent obtained from each patient.

Statistics:

Means of all groups were compared for statistical differences by Student *t* test or a One-Way Analysis of Variance (ANOVA). A Bonferroni *t* test was used, following the ANOVA, to understand the statistical difference between two groups, when more than two groups were compared. Data was presented as means ± SD. Significance levels were set to $P < 0.05$.

Results

$CD8^+$ Suppressor TILs in the human tumor microenvironment.

Patients with tumors have increased numbers of $CD27^-/CD28^-$ $CD8^+$ T cells in the periphery and in the tumor microenvironment (14,19). The $CD8^+$ T cells in the tumor microenvironment express multiple immune checkpoint proteins, including PD-1 and Tim-3 (1–4). We investigated whether these populations are actually the same dysfunctional T cells. Fifteen freshly-obtained tumor specimens (eight HPV-positive or -negative head and neck tumors, and seven melanoma tumors) were dissociated into tumor cell/ T-cell suspensions, stained for surface marker expression and analyzed by flow cytometry (20). Figure 1A summarizes the expression of CD27, CD28, PD-1, and Tim-3 by the $CD8^+$ T cells from SCCHN and melanoma patients. Memory marker staining of these cells can be found in Supplementary Fig. S2A and show that the majority are of a $CCR7^-$ $CD45RA^-$ effector/memory phenotype. Tumor-derived $CD8^+$ cells express less CD27 and CD28 and

more PD-1 and Tim-3 than peripheral blood lymphocytes from the same patients (Fig. 1B). Tumor-derived T cells from these patients included overlapping populations of $CD27^{-}$ $CD28^{-}$ and multi-checkpoint^{+} expressing cells (Fig. 1C), thus these two independently characterized tumor-associated T-cell populations are predominantly one and the same.

When normal human T cells are cocultured *in vitro* with a variety of individual human tumor cell lines, the lymphocytes lose their CD27 and CD28 expression, become dysfunctional, and acquire the capacity to suppress effector T cells (12,13). $CD28^{-}$ $CD8^{+}$ T-cells isolated from various cancers are suppressive, as well (14). Here we tested whether isolated tumor-infiltrating $CD8^{+}$ T cells from patients could also act as suppressor cells. We purified $CD27^{-}$ $CD28^{-}$ $CD8^{+}$ cells (Fig. 1D) or PD-1^{+} Tim-3^{+} $CD8^{+}$ T cells (Fig. 1E) from human SCCHN tumors by automated cell sorting, then used the cells in a suppression assay with $CD3^{+}$ responder T cells isolated from the peripheral blood of the same patients. Thus the tumor-derived $CD8^{+}$ TILs were suppressive even when incubated at suppressor to responder ratios as low as 1:5. We performed similar suppression studies using PD-1^{+} Tim-3^{+} $CD8^{+}$ TILs and proliferation was assessed by CFSE dilution or BrdU uptake (Fig. 1F). Suppression of responder T cells was observed at lower ratios similar to tritium-uptake studies. Thus $CD8^{+}$ patient TILs, which are both $CD27^{-}$-$CD28^{-}$ and PD-1^{+} Tim-3^{+}, are similarly suppressive. Given that suppressive dysfunctional T cells can be induced by tumor lines *in vitro* in the absence of antigen recognition, our results imply that tumor-derived factors alone can stimulate expression of immune checkpoint proteins and reduce T-cell function.

A mouse model of $CD8^{+}$ TIL suppression in SCCHN.

The TC-1 tumor cell line served as our murine model of SCC to further assess the role of $CD8^{+}$ TIL-mediated suppression. These cells were created by expressing human papilloma virus (HPV) E6 and E7 proteins in mouse cells, which drives a carcinogenesis process similar to human SCCHN (21). Unlike human T cells, which lose CD27and CD28 expression in the tumor microenvironment or when exposed to SCCHN tumors *in vitro*, mouse cells do not. However, both human and murine $CD8^{+}$ T cells are induced to elevate expression of PD-1 after co-incubation with their species-specific tumor cell line when separated by a transwell insert and in the absence of any activation (Fig. 2A). Murine $CD8^{+}$ T cells cocultured with TC-1 become as suppressive as tumor-exposed human T cells, rendering them capable of inhibiting the proliferation of normal, syngeneic T cells incubated on anti-CD3/anti-CD28-coated plates or with allogeneic stimulator cells (Fig. 2B)(12). Similar results were obtained using murine tumor cell lines B16 and EL4, indicating that this phenomenon is not specific to TC-1 cells. Analogous results were observed when we characterized the murine $CD8^{+}$ TILs purified from TC-1 tumors. Tumor tissue isolated from TC-1-bearing mice was dissociated and the expression of checkpoint proteins by murine TILs was assessed by flow cytometry. Murine $CD8^{+}$ T cells infiltrating TC-1 tumors overexpressed PD-1 and Tim-3 with most of the $CD8^{+}$ TILs expressing both markers (Fig. 2C). Memory marker expression by these cells was also assessed and found the majority to be $CD44^{+}$ $CD62L^{-}$, a phenotype associated with memory/effector cells (Supplementary Fig. S2B). We next assessed the ability of $CD8^{+}$ TILs from mouse tumors to suppress the function of normal $CD8^{+}$ T cells using *ex vivo* coculture assays. The majority of $CD8^{+}$ TILs sorted from TC-1 tumor digests were PD-1^{+} Tim-3^{+} and able to suppress the proliferation of

naïve, syngeneic responder T cells (Fig. 2D). As in our previous *ex vivo* human suppression studies, we observed significant suppression of responder T cells using CFSE dilution and BrdU uptake (Fig. 2E). The $CD8^+$ TILs fell into three distinct populations with respect to PD-1 and Tim-3 expression ($PD\text{-}1^-$ $Tim\text{-}3^-$, $PD\text{-}1^+$ $Tim\text{-}3^-$, and $PD\text{-}1^+$ $Tim\text{-}3^+$) (Fig. 2F). When the three purified populations were compared following FACS sorting, only the $PD\text{-}1^+$ $Tim\text{-}3^+$ $CD8^+$ T cells could inhibit T-cell function, whether measured by ^{3}H-thymidine uptake, CFSE dilution, or BrdU uptake (Fig. 2F, G). Because the number of cells available from unexpanded human specimen TILs (even from large tumors) is so limited, we were unable to perform the parallel experiments with this precious resource.

Checkpoint inhibitor blockade decreased suppression by TILs and enhanced antitumor immunity.

Signaling through checkpoint proteins inhibits T-cell function, and antibodies that bind to and block these negative regulators drive clinical responses (22,23). We assessed $PD\text{-}1^+$ $Tim\text{-}3^+$ $CD8^+$ T-cell suppressive abilities using PD-1 and Tim-3 blocking antibodies. We show that *in vitro* anti-PD-1 treatment significantly blocked the suppressive effects of these TILs in *ex vivo* coculture suppression assays (Fig. 3A). With the same treatment *in vivo,* antibody blockade of PD-1 and Tim-3 each significantly slowed TC-1 tumor growth as compared to no treatment or an IgG control (Fig. 3B). Neither antibody treatment affected the percentage of $PD\text{-}1^+$ and/or $Tim\text{-}3^+$ expressing TILs (Fig. 3C). These antibodies in other mouse tumor models promote $CD8^+$ T-cell interferon-gamma (IFNγ) production and cytotoxic activity, leading to an enhanced antitumor effect (24–26). We similarly found that blockade of either PD-1 or Tim-3 caused $CD8^+$ TILs to produce more IFNγ when re-stimulated with either anti-CD3/CD28 or irradiated TC-1 tumor cells (Fig. 3D). Checkpoint blockade antibodies significantly reduced the suppressive potential of $PD\text{-}1^+$ $Tim\text{-}3^+$ $CD8^+$ TILs sorted from treated mice (Fig. 3E). These data suggest that the ability of checkpoint inhibitor blockade to augment antitumor immune responses results from both the enhancement of $CD8^+$ T-cell function and by blocking the development of suppressive function. That the reversal of suppression occurred after *in vivo* use of the antibodies further suggests a benefit of checkpoint inhibition lies in preventing the development of suppressive function rather than blocking an already developed suppressive function.

IL7 treatment synergizes with checkpoint-inhibitor blockade.

Although checkpoint inhibitors have revolutionized cancer therapy, therapies build on combination strategies bring added potential. In our *in vitro* model of tumor-induced T-cell dysfunction, IL7 protected human T cells from CD27 and CD28 loss and induction of suppression abilities (13). Having observed that antibody checkpoint-inhibitor blockade could also reduce the suppressive ability of $PD\text{-}1^+$ $Tim\text{-}3^+$ $CD8^+$ TIL, we combined these two treatment strategies to determine if a synergistic effect took place. In our previous study, we observed that in the peripheral blood of cancer patients, loss of CD27 and CD28 expression was accompanied by the loss of CD127 (IL7rα). Therefore we assessed the expression of CD127 on $CD8^+$ TILs present in human tumors. Indeed, we observed that expression of PD-1 and Tim-3 on human tumor TIL specimens was accompanied by the lack of CD127. (Fig. 4A). Likewise, $CD8^+$ TILs isolated from TC-1 tumors demonstrate a similar pattern, in which gain of PD-1 and Tim-3 expression associates with the loss of CD127.

(Fig. 4B). Together, these data indicate that multi-checkpoint expressing $CD8^+$ T-cell populations also lack CD127 expression in both mouse and human tumors. Before embarking on a combination strategy, we analyzed CD127 expression on $CD8^+$ TILs from the antibody blockade experiments in Fig. 3 and found significantly increased expression of CD127 on antibody-treated T cells (Fig. 4C). We then combined IL7 treatment with anti-PD-1 therapy and observed an additive effect in our *in vivo* TC-1 tumor model. Similar to earlier mouse studies, anti-PD-1 blockade was also initiated on day 7 The combination of IL7 with anti-PD-1 treatment resulted in a significant reduction in tumor growth as compared to each treatment alone (Fig. 4D). Anti-PD-1 treatment alone was more effective than IL7 cytokine treatment alone. At the conclusion of the experiment, expression of PD-1 and Tim-3 on $CD8^+$ TILs was assessed by flow cytometry. Like our previous antibody blockade studies, $CD8^+$ TILs in all treatment groups displayed elevated expression of both PD-1 and Tim-3 similar to control TC-1 tumors (Fig. 4E). Also similar to previous studies using antibody blockade alone, $PD\text{-}1^+$ $Tim3^+$ $CD8^+$ TILs from treatment groups receiving anti-PD-1 displayed greater IFNγ production upon restimulation and significantly reduced suppressive ability when used in *ex vivo* suppression assays (Fig. 4F-G). Although the combination of IL7 and anti-PD-1 resulted in the greatest delay in tumor growth *in vivo*, the combination's improvement over anti-PD-1 alone was not observed in *ex vivo* analyses. These findings are likely due to other immune-promoting activities of IL7 that were not assessed or were transient, but that are promoted by anti-PD-1 up-regulating the IL7 receptor.

Adoptive T-cell transfer synergizes with checkpoint-inhibitor blockade.

Another combinational strategy under investigation is checkpoint inhibition with various types of adoptive immune cell transfer, such as antigen-specific T cells. To develop a model of adoptive T-cell therapy in SCCHN, we obtained mice engineered to express a TCR-β chain that recognizes the HPV E7 epitope presented by $H2\text{-}D^b$ (E7-T). These transgenic TCR-β chains combine with random endogenous α-chains to form a repertoire of T cells with varying avidities towards the E7 epitope (Supplementary Fig. S3A) (15). We then bred a Thy1.1 congenic marker onto these E7-TCRβ transgenic T cells to facilitate the tracking of these cells after adoptive transfer and verified that they are able to lyse TC-1 tumor cells in an *in vitro* assay (Supplementary Fig. S3B). We next adoptively transferred increasing numbers of these E7-T cells in mice bearing TC-1 showing a dose response as larger numbers of antigen specific T cells resulted in greater abrogation of tumor growth (Supplementary Fig. S3C). Memory marker staining of E7-T cells used in adoptive transfer experiments can be found in Supplementary Fig. S3D. Clinical trials using antigen specific T cells as a monotherapy resulted in modest clinical effects in patients.(27–29) Thus we chose for adoptive T cell therapy a number of cells that produced measurable but mild antitumor responses, which was 1×10^6 cells.

When we combined adoptive transfer of the E7-T cells together with anti-PD-1, we found that the combination synergized to inhibit tumor growth (Fig. 5A). When excised and digested $CD8^+$ TILs from treated tumors were stained for the Thy 1.1 congenic marker, those from mice treated with anti-PD-1 were found to contain a greater percentage of the transferred E7-T $CD8^+$ cells than tumors from mice that were injected with IgG control

antibodies (Fig. 5B). Endogenous TILs ($CD8^+$/$Thy1.1^-$) from both treatment groups displayed high PD-1 and Tim-3 expression comparable to the IgG control. (Fig. 5C). Also similar to endogenous cells, a higher percentage of Thy 1.1^+ $CD8^+$ TILs in PD-1 treated mice produced IFNγ upon *ex vivo* restimulation with anti-CD3/CD28 (Fig. 5D). Likewise, we found that transferred (Thy1.1 expressing) PD-1^+ Tim-3^+ $CD8^+$ T cells from TC-1 tumors underwent a similar conversion to suppressor T cell (Fig. 5E). Thus, checkpoint blockade maintains $CD8^+$ T-cell function and enhances antigen-specific T-cell infiltration into the tumor microenvironment, both of which enhance antitumor effects.

Ex vivo blockade of checkpoint inhibitors reduces suppressive function of patient $CD8^+$ TIL.

We then examined whether the treatment with checkpoint blockade could reduce the suppressive function of human tumor-derived $CD8^+$ suppressive T cells *ex vivo*. PD-1^+ Tim-3^+ $CD8^+$ TILs were sorted and purified from either human SCCHN or melanoma tumors, and, without expansion or treatment, were incubated with autologous responder PBMC T cells. These cocultures were treated with combinations of anti-human-PD-1 and anti-Tim-3 blocking antibodies. As in the mouse model, we found that blockade of these two checkpoint inhibitors reduced the suppressive function of the human PD-1^+ Tim-3^+ $CD8^+$ TILs, whereas the IgG control antibodies had no effect (Fig. 6A-B). Similar suppression results were observed when responder proliferation was assessed by CFSE dilution and BrdU incorporation (Fig. 6C). As part of these studies, we also assessed the expression of PD-1 and Tim-3 on the responder T cells from mice and humans used in these studies and found very low baseline expression on these cells, suggesting that the initial benefit of *in vitro* blockade would come from blocking the PD-1 and Tim-3 on the suppressor T cells (Supplementary Fig. S4). Along with the similar data using mouse TIL, these results indicate that checkpoint blockade reduced the suppressive ability of PD-1^+ Tim-3^+ $CD8^+$ TIL. However, the relationship between the beneficial effects of blocking $CD8^+$ TIL checkpoint molecules *ex vivo* to any clinically therapeutic advantage remains to be studied. Finally, our data suggest that these PD-1^+ Tim-3^+ positive $CD8^+$ T cells continue to be suppressive without active tumor interaction.

$CD8^+$ TILs express ligands for PD-1 and Tim-3

Since we observed that antibody blockade (*ex vivo*) of PD-1 and to a lesser extent Tim-3 could reduce the suppressive function of $CD8^+$ T cells, we wanted to know if the suppressive $CD8^+$ T cells were the source of checkpoint ligand expression. Although expression of the ligands for PD-1 and Tim-3 (primarily PD-L1 and galectin-9, respectively) are known on non-$CD8^+$ T-cell immune populations within the tumor microenviroment, such as $CD4^+$ Treg, various macrophage and dendritic cell populations, and the tumor cells themselves (staining for TC-1 tumors can be found in Supplementary Fig. S5), the *ex vivo* suppression assays do not contain these cells.(24,30,31) We assessed expression of PD-L1 and galectin-9 with PD-1 and Tim-3 expression on $CD8^+$ T cells from both spleen and dissociated TC-1 tumors of C57BL/6 mice (Fig. 7A-C). Tumor-resident $CD8^+$ cells highly expressed PD-L1 regardless of PD-1 expression, whereas normal spleen $CD8^+$ T cells had low expression of PD-L1 even on PD-1^+ or Tim-3^+ cells Galectin-9 expression positively correlated with both PD-1 and Tim-3 expression. The association between galectin-9 and Tim-3 expression was

also observed in the spleen. We then performed similar studies on TILs from dissociated human tumor tissue specimens and normal donor PBMCs (Fig. 7D-F). Like tumor-resident $CD8^+$ T cells in murine tumors, human $CD8^+$ TILs highly expressed of PD-L1 on both $PD\text{-}1^+$ and $Tim\text{-}3^+$ T cells. However, human $CD8^+$ TILs had a much smaller population that expressed galectin-9, though most cells that expressed this ligand were also $PD\text{-}1^+$ and $Tim\text{-}3^+$. PBMCs did not show the correlation between checkpoints and their respective ligands seen in TILs. In this the human and murine tumors differ, consistent with the fact that anti-Tim-3 treatment was only effective in the murine *ex vivo* experiments. We did not observe significant PD-L2 staining on either mouse or human T cells. Together these data indicate that suppressive tumor-resident $CD8^+$ T cells also express the ligands to checkpoint markers such as PD-1 and Tim-3, suggesting that signaling through these receptors may be initiated by a variety of cell types, including the T cells themselves. Whether autocrine signaling through these receptors on the suppressive $CD8^+$ TILs, or paracrine signaling to nearby effector $CD8^+$ T cells, plays a key role in their development or function remains incompletely understood, however our previous data on blockade of these receptors in *ex vivo* suppression studies suggests that this signaling route may be physiologically relevant.

$CD8^+$ TILs exert suppressive function through a mechanism involving IL10 and cell contact

We sought to determine a mechanism by which $CD8^+$ TILs exert their suppressive effect on nearby T cells. To determine whether neutralizing antibodies to common regulatory cytokines could reduce or reverse the suppressive effect we observe in *ex vivo* suppression assays, we added blocking antibodies (10ug/ml) against IL6, IL10, and TGFβ to the suppression assays using $PD\text{-}1^+$ $Tim\text{-}3^+$ TILs FACS-sorted from TC-1 tumors (Fig. 8A). Of the tested antibodies, we found that only neutralization of IL10 led to a significant restoration of the proliferation of responder T cells, as measured by CFSE dilution or BrdU incorporation. Similar results were obtained with $PD\text{-}1^+$ $Tim\text{-}3^+$ TILs sorted from human tumors (Fig. 8B). Intracellular cytokine staining of stimulated $PD\text{-}1^+$ $Tim\text{-}3^+$ $CD8^+$ T cells found production of IL10 by these cells (Supplementary Fig. S6). These data suggest that IL10 secretion by $CD8^+$ TILs mediates the suppressive effect of these cells. Previous studies on both $CD4^+$ and $CD8^+$ suppressive T-cell populations have found that cell to cell contact is important for the suppressive effect.(32,33) Indeed, our previous work with *in vitro*–derived, tumor-induced suppressive T cells found that cell contact was required, as the separation of responders and suppressors via transwell inserts prevented the suppression of responder proliferation.(12) To this end we conducted suppressive assays using transwell inserts to separate sorted $PD\text{-}1^+$ $Tim\text{-}3^+$ $CD8^+$ T cells from responder T cells seeded in antibody-coated plates (Fig. 8C). In assays using both mouse and human T cells, we found that physical separation prevented suppression. Together these data suggest that the suppression mediated by $PD\text{-}1^+$ $Tim\text{-}3^+$ $CD8^+$ TILs requires both IL10 and cell-contact.

Discussion

$CD8^+$ regulatory cells are part of the immunosuppressive network of the tumor microenvironment (34). $CD8^+$ TILs can lose cytotoxic function and become capable of suppressing other T cells in *ex vivo* assays, and greater numbers of $CD8^+$ TILs correlate with disease progression and worse prognosis(14,35,36). Work from our lab suggests that

soluble, tumor-derived factors induce dysfunction in $CD8^+$ T cells (12,13). Here we correlate PD-1 and Tim-3 to CD27/CD28 loss in and suppression of $CD8^+$ T cells in the context of cancer. We show that in human and mouse models $CD8^+$ suppressor function is abrogated by blocking PD-1 and Tim-3.

Here we combined anti-PD-1 with IL7, a cytokine we previously showed could help T cells resist dysfunction (13). As a single agent, IL7 has shown activity in mouse tumor models, though in human patients, only a slight overall clinical benefit was observed (37–39). That IL7 and anti-PD-1 affect different receptors and have distinct effects argues for their combination in the clinic. Indeed, these two therapies synergize in a sepsis model of immunosuppression (40).

Our data in adoptive T-cell therapy shows the value of blocking $CD8^+$ suppressor development. We show that TCR transgenic $CD8^+$ T-cells that should act as antitumor agents indeed become enriched in the tumor but also develop the dysfunctional and suppressive features of native TIL. This may explain why treating patients with interventions intended to boost T-cell function, such as antigen specific T-cell therapy or vaccines designed to expand cytotoxic cells, may not eliminate solid tumors (41,42). In fact, PD-1 expression or CD27 and CD28 loss have negative effects on transferred T cells (43,44). Our findings now suggest that checkpoint-inhibitor blockade could optimize adoptive-cell therapy regimens by both maintaining T-cell cytotoxic function and preventing acquisition of immunosuppressive characteristics.

We found that PD-1/Tim-3 checkpoint positive $CD8^+$ T cells from both mouse and human tumors expressed excess PD-L1. The same T cells also expressed excess galectin-9, though not at the same level in human tumors. It is possible that this phenomenon likely varies from patient to patient. The fact that blocking Tim-3 was only effective for preventing suppressive function *in vivo* suggests that there is a required threshold of expression of galectin-9. In the tumor microenvironment, where galectin-9 expression is abundant, this threshold would be reached, rendering anti-Tim-3 therapy more effective (4,24,45). An alternative explanation is that there are other less characterized ligands for Tim-3 that may not be expressed by $CD8^+PD\text{-}1^+Tim\text{-}3^+$ cells such as phosphatidylserine, a known Tim-3 ligand highly expressed on tumor cells (46).

Our data with *in vitro* treatment with anti-PD-1 of mouse and human TILs may explain why PD-L1 expression is not always observed on the cancer cells of patients who respond to this type of therapy (47). Here the PD-1/PD-L1 interaction responsible for regulating the antitumor T-cell response would be mediated by $PD\text{-}L1^+$ TIL. Thus the use of PD-L1 expression by tumor cells as a clinical biomarker to identify patients for anti-PD-1 therapy may exclude some patients who would nonetheless respond to anti-PD-1 therapy (48–50).

Using neutralizing antibodies, we found that $PD\text{-}1^+$ $Tim3^+$ $CD8^+$ TILs from both mouse and human tumor tissues exert their suppressive function via the production of IL10 and require cell contact. The cytokine IL10 regulates cytotoxic T-cell responses in cancer(51,52). IL10 producing $CD8^+$ T cells are negative regulators of T-cell responses, particularly in autoimmune, viral infection models and in tumor microenvironments(33,53,54). IL10 also

plays a role in immune stimulation, as it is required for helper-T-cell function and in some cases with positive antitumor immune responses (53,55). Conversely, PD-1 signaling potentiates expression of the IL10 receptor by tumor-associated $CD8^+$ T cells, which downregulates their cytotoxic activity (53). Thus, while exogenous super-physiologic administration of IL10 may augment immune function, blocking it at the tumor/local level could reduce suppression mediated by $CD8^+$ TILs and other regulatory cells. Our observation that $CD8^+$ TIL–mediated suppression requires both IL10 and cell contact suggests that this effect may be limited to the immediate microenvironment around the suppressive cells, perhaps even requiring trans-presentation similar to IL15. In this case, suppression occurs either in addition to, or in concert with PD-L1/PD-1 signaling, as shown by the lack of baseline PD-1 and Tim-3 on the responder cells used in our suppression studies.

In our TC-1 mouse tumor model, we found expression of PD-1 and Tim-3 ligands on tumor cells under both *in vitro* and *in vivo* growth conditions. These observations suggest that signaling through these receptors in the tumor microenvironment involves interaction with both immune and tumor cells. In addition to enhanced checkpoint-ligand expression, studies from our lab revealed that tumor-derived exosomes drive generation of $PD\text{-}1^+$ $CD8^+$ suppressor cells (56). Together, these observations suggest that the presence and function of $CD8^+$ suppressive TILs is a consequence of a network of signals. The relative contribution of each of these components is the subject of ongoing study by our group.

In summary, our data reveal a tumor-induced $CD8^+$ T-cell suppressor population that is a target of modern checkpoint-based immunotherapy. The determination that these suppressor cells are $CD8^+$ $CD27^-$ $CD28^-$ multi-checkpoint $inhibitor^+$ not only reconciles data from studies of immune effector dysfunction, but also increases our understanding of how checkpoint blockade mediates its effects. Our results from patients' samples were only made possible by collaborative efforts to obtain large volume tumors, which yielded enough TILs to do functional assays without expanding T cells. The conclusions from this work not only provide insight into targets of checkpoint blockade, but also suggest the value of combining of this form of immunotherapy with other strategies to optimize clinical outcomes.

Supplementary Material

Refer to Web version on PubMed Central for supplementary material.

Acknowledgments

This work was supported by NIH grant R01CA132796 (to B.R.G.)

References

1. Tumeh PC, Harview CL, Yearley JH, Shintaku IP, Taylor EJ, Robert L, et al. PD-1 blockade induces responses by inhibiting adaptive immune resistance. Nature 2014;515(7528):568–71 doi 10.1038/nature13954. [PubMed: 25428505]
2. Pardoll DM. The blockade of immune checkpoints in cancer immunotherapy. Nat Rev Cancer 2012;12(4):252–64 doi 10.1038/nrc3239. [PubMed: 22437870]

3. Tsushima F, Yao S, Shin T, Flies A, Flies S, Xu H, et al. Interaction between B7-H1 and PD-1 determines initiation and reversal of T-cell anergy. Blood 2007;110(1):180–5 doi 10.1182/blood-2006-11-060087. [PubMed: 17289811]

4. Sakuishi K, Apetoh L, Sullivan JM, Blazar BR, Kuchroo VK, Anderson AC. Targeting Tim-3 and PD-1 pathways to reverse T cell exhaustion and restore anti-tumor immunity. J Exp Med 2010;207(10):2187–94 doi 10.1084/jem.20100643. [PubMed: 20819927]

5. Goldberg P FDA Eager to Approve PD-1 and PD-L1 Drugs in Novel Combinations, New Settings The Cancer Letter 2016 11 11, 2016:1–6.

6. Siegel RL, Miller KD, Jemal A. Cancer statistics, 2015. CA Cancer J Clin 2015;65(1):5–29 doi 10.3322/caac.21254. [PubMed: 25559415]

7. Ang KK, Harris J, Wheeler R, Weber R, Rosenthal DI, Nguyen-Tan PF, et al. Human papillomavirus and survival of patients with oropharyngeal cancer. N Engl J Med 2010;363(1):24–35 doi 10.1056/NEJMoa0912217. [PubMed: 20530316]

8. Li Q, Prince ME, Moyer JS. Immunotherapy for head and neck squamous cell carcinoma. Oral Oncol 2015;51(4):299–304 doi 10.1016/j.oraloncology.2014.12.005. [PubMed: 25624094]

9. Trosman SJ, Koyfman SA, Ward MC, Al-Khudari S, Nwizu T, Greskovich JF, et al. Effect of human papillomavirus on patterns of distant metastatic failure in oropharyngeal squamous cell carcinoma treated with chemoradiotherapy. JAMA Otolaryngol Head Neck Surg 2015;141(5):457–62 doi 10.1001/jamaoto.2015.136. [PubMed: 25742025]

10. Gentzler R, Hall R, Kunk PR, Gaughan E, Dillon P, Slingluff CL Jr., et al. Beyond melanoma: inhibiting the PD-1/PD-L1 pathway in solid tumors. Immunotherapy 2016;8(5):583–600 doi 10.2217/imt-2015-0029. [PubMed: 27140411]

11. Mahoney KM, Freeman GJ, McDermott DF. The Next Immune-Checkpoint Inhibitors: PD-1/PD-L1 Blockade in Melanoma. Clin Ther 2015;37(4):764–82 doi 10.1016/j.clinthera.2015.02.018. [PubMed: 25823918]

12. Montes CL, Chapoval AI, Nelson J, Orhue V, Zhang X, Schulze DH, et al. Tumor-induced senescent T cells with suppressor function: a potential form of tumor immune evasion. Cancer Res 2008;68(3):870–9 doi 10.1158/0008-5472.CAN-07-2282. [PubMed: 18245489]

13. Zhang Y, Pfannenstiel LW, Bolesta E, Montes CL, Zhang X, Chapoval AI, et al. Interleukin-7 inhibits tumor-induced CD27-CD28- suppressor T cells: implications for cancer immunotherapy. Clin Cancer Res 2011;17(15):4975–86 doi 10.1158/1078-0432.CCR-10-3328. [PubMed: 21712448]

14. Filaci G, Fenoglio D, Fravega M, Ansaldo G, Borgonovo G, Traverso P, et al. CD8+ CD28- T regulatory lymphocytes inhibiting T cell proliferative and cytotoxic functions infiltrate human cancers. J Immunol 2007;179(7):4323–34. [PubMed: 17878327]

15. Narayan S, Choyce A, Linedale R, Saunders NA, Dahler A, Chan E, et al. Epithelial expression of human papillomavirus type 16 E7 protein results in peripheral CD8 T-cell suppression mediated by CD4+CD25+ T cells. Eur J Immunol 2009;39(2):481–90 doi 10.1002/eji.200838527. [PubMed: 19180468]

16. Chen CH, Suh KW, Ji H, Choti MA, Pardoll DM, Wu TC. Antigen-specific immunotherapy for human papillomavirus 16 E7-expressing tumors grown in the liver. J Hepatol 2000;33(1):91–8. [PubMed: 10905591]

17. Hirano F, Kaneko K, Tamura H, Dong H, Wang S, Ichikawa M, et al. Blockade of B7-H1 and PD-1 by monoclonal antibodies potentiates cancer therapeutic immunity. Cancer research 2005;65(3):1089–96. [PubMed: 15705911]

18. Anderson AC, Anderson DE, Bregoli L, Hastings WD, Kassam N, Lei C, et al. Promotion of tissue inflammation by the immune receptor Tim-3 expressed on innate immune cells. Science 2007;318(5853):1141–3 doi 10.1126/science.1148536. [PubMed: 18006747]

19. Karagoz B, Bilgi O, Gumus M, Erikci AA, Sayan O, Turken O, et al. CD8+CD28- cells and CD4+CD25+ regulatory T cells in the peripheral blood of advanced stage lung cancer patients. Med Oncol 2010;27(1):29–33 doi 10.1007/s12032-008-9165-9. [PubMed: 19148592]

20. Weiss VL, Lee TH, Song H, Kouo TS, Black CM, Sgouros G, et al. Trafficking of high avidity HER-2/neu-specific T cells into HER-2/neu-expressing tumors after depletion of effector/memory-

like regulatory T cells. PLoS One 2012;7(2):e31962 doi 10.1371/journal.pone.0031962. [PubMed: 22359647]

21. Narisawa-Saito M, Kiyono T. Basic mechanisms of high-risk human papillomavirus-induced carcinogenesis: roles of E6 and E7 proteins. Cancer Sci 2007;98(10):1505–11 doi 10.1111/j.1349-7006.2007.00546.x. [PubMed: 17645777]
22. Topalian SL, Hodi FS, Brahmer JR, Gettinger SN, Smith DC, McDermott DF, et al. Safety, activity, and immune correlates of anti-PD-1 antibody in cancer. N Engl J Med 2012;366(26):2443–54 doi 10.1056/NEJMoa1200690. [PubMed: 22658127]
23. Hodi FS, O'Day SJ, McDermott DF, Weber RW, Sosman JA, Haanen JB, et al. Improved survival with ipilimumab in patients with metastatic melanoma. N Engl J Med 2010;363(8):711–23 doi 10.1056/NEJMoa1003466. [PubMed: 20525992]
24. Fourcade J, Sun Z, Benallaoua M, Guillaume P, Luescher IF, Sander C, et al. Upregulation of Tim-3 and PD-1 expression is associated with tumor antigen-specific CD8+ T cell dysfunction in melanoma patients. J Exp Med 2010;207(10):2175–86 doi 10.1084/jem.20100637. [PubMed: 20819923]
25. Duraiswamy J, Kaluza KM, Freeman GJ, Coukos G. Dual blockade of PD-1 and CTLA-4 combined with tumor vaccine effectively restores T-cell rejection function in tumors. Cancer Res 2013;73(12):3591–603 doi 10.1158/0008-5472.CAN-12-4100. [PubMed: 23633484]
26. Ngiow SF, von Scheidt B, Akiba H, Yagita H, Teng MW, Smyth MJ. Anti-TIM3 antibody promotes T cell IFN-gamma-mediated antitumor immunity and suppresses established tumors. Cancer Res 2011;71(10):3540–51 doi 10.1158/0008-5472.CAN-11-0096. [PubMed: 21430066]
27. Morgan RA, Dudley ME, Wunderlich JR, Hughes MS, Yang JC, Sherry RM, et al. Cancer regression in patients after transfer of genetically engineered lymphocytes. Science 2006;314(5796):126–9 doi 10.1126/science.1129003. [PubMed: 16946036]
28. Yong CSM, Dardalhon V, Devaud C, Taylor N, Darcy PK, Kershaw MH. CAR T-cell therapy of solid tumors. Immunol Cell Biol 2017;95(4):356–63 doi 10.1038/icb.2016.128. [PubMed: 28003642]
29. Rosenberg SA, Yang JC, Sherry RM, Kammula US, Hughes MS, Phan GQ, et al. Durable complete responses in heavily pretreated patients with metastatic melanoma using T-cell transfer immunotherapy. Clin Cancer Res 2011;17(13):4550–7 doi 10.1158/1078-0432.CCR-11-0116. [PubMed: 21498393]
30. Ahmadzadeh M, Johnson LA, Heemskerk B, Wunderlich JR, Dudley ME, White DE, et al. Tumor antigen-specific CD8 T cells infiltrating the tumor express high levels of PD-1 and are functionally impaired. Blood 2009;114(8):1537–44 doi 10.1182/blood-2008-12-195792. [PubMed: 19423728]
31. Marcq E, Waele J, Audenaerde JV, Lion E, Santermans E, Hens N, et al. Abundant expression of TIM-3, LAG-3, PD-1 and PD-L1 as immunotherapy checkpoint targets in effusions of mesothelioma patients. Oncotarget 2017;8(52):89722–35 doi 10.18632/oncotarget.21113. [PubMed: 29163783]
32. Muthu Raja KR, Kubiczkova L, Rihova L, Piskacek M, Vsianska P, Hezova R, et al. Functionally suppressive CD8 T regulatory cells are increased in patients with multiple myeloma: a cause for immune impairment. PLoS One 2012;7(11):e49446 doi 10.1371/journal.pone.0049446. [PubMed: 23152910]
33. Endharti AT, Rifa IM, Shi Z, Fukuoka Y, Nakahara Y, Kawamoto Y, et al. Cutting edge: CD8+CD122+ regulatory T cells produce IL-10 to suppress IFN-gamma production and proliferation of CD8+ T cells. J Immunol 2005;175(11):7093–7. [PubMed: 16301610]
34. Reiser J, Banerjee A. Effector, Memory, and Dysfunctional CD8(+) T Cell Fates in the Antitumor Immune Response. J Immunol Res 2016;2016:8941260 doi 10.1155/2016/8941260. [PubMed: 27314056]
35. Onyema OO, Decoster L, Njemini R, Forti LN, Bautmans I, De Waele M, et al. Shifts in subsets of CD8+ T-cells as evidence of immunosenescence in patients with cancers affecting the lungs: an observational case-control study. BMC Cancer 2015;15:1016 doi 10.1186/s12885-015-2013-3. [PubMed: 26711627]
36. Filaci G, Fravega M, Negrini S, Procopio F, Fenoglio D, Rizzi M, et al. Nonantigen specific CD8+ T suppressor lymphocytes originate from CD8+CD28- T cells and inhibit both T-cell proliferation

and CTL function. Hum Immunol 2004;65(2):142–56 doi 10.1016/j.humimm.2003.12.001. [PubMed: 14969769]

37. Klebanoff CA, Gattinoni L, Palmer DC, Muranski P, Ji Y, Hinrichs CS, et al. Determinants of successful CD8+ T-cell adoptive immunotherapy for large established tumors in mice. Clin Cancer Res 2011;17(16):5343–52 doi 10.1158/1078-0432.CCR-11-0503. [PubMed: 21737507]
38. Sportes C, Babb RR, Krumlauf MC, Hakim FT, Steinberg SM, Chow CK, et al. Phase I study of recombinant human interleukin-7 administration in subjects with refractory malignancy. Clin Cancer Res 2010;16(2):727–35 doi 10.1158/1078-0432.CCR-09-1303. [PubMed: 20068111]
39. Rosenberg SA, Sportes C, Ahmadzadeh M, Fry TJ, Ngo LT, Schwarz SL, et al. IL-7 administration to humans leads to expansion of CD8+ and CD4+ cells but a relative decrease of CD4+ T-regulatory cells. J Immunother 2006;29(3):313–9 doi 10.1097/01.cji.0000210386.55951.c2. [PubMed: 16699374]
40. Shindo Y, Unsinger J, Burnham CA, Green JM, Hotchkiss RS. Interleukin-7 and anti-programmed cell death 1 antibody have differing effects to reverse sepsis-induced immunosuppression. Shock 2015;43(4):334–43 doi 10.1097/SHK.0000000000000317. [PubMed: 25565644]
41. Kunert A, Straetemans T, Govers C, Lamers C, Mathijssen R, Sleijfer S, et al. TCR-Engineered T Cells Meet New Challenges to Treat Solid Tumors: Choice of Antigen, T Cell Fitness, and Sensitization of Tumor Milieu. Front Immunol 2013;4:363 doi 10.3389/fimmu.2013.00363. [PubMed: 24265631]
42. van der Burg SH, Arens R, Ossendorp F, van Hall T, Melief CJ. Vaccines for established cancer: overcoming the challenges posed by immune evasion. Nat Rev Cancer 2016;16(4):219–33 doi 10.1038/nrc.2016.16. [PubMed: 26965076]
43. Cherkassky L, Morello A, Villena-Vargas J, Feng Y, Dimitrov DS, Jones DR, et al. Human CAR T cells with cell-intrinsic PD-1 checkpoint blockade resist tumor-mediated inhibition. J Clin Invest 2016;126(8):3130–44 doi 10.1172/JCI83092. [PubMed: 27454297]
44. Powell DJ Jr., Dudley ME, Robbins PF, Rosenberg SA. Transition of late-stage effector T cells to CD27+ CD28+ tumor-reactive effector memory T cells in humans after adoptive cell transfer therapy. Blood 2005;105(1):241–50 doi 10.1182/blood-2004-06-2482. [PubMed: 15345595]
45. Zhou Q, Munger ME, Veenstra RG, Weigel BJ, Hirashima M, Munn DH, et al. Coexpression of Tim-3 and PD-1 identifies a CD8+ T-cell exhaustion phenotype in mice with disseminated acute myelogenous leukemia. Blood 2011;117(17):4501–10 doi 10.1182/blood-2010-10-310425. [PubMed: 21385853]
46. Freeman GJ, Casasnovas JM, Umetsu DT, DeKruyff RH. TIM genes: a family of cell surface phosphatidylserine receptors that regulate innate and adaptive immunity. Immunol Rev 2010;235(1):172–89 doi 10.1111/j.0105-2896.2010.00903.x. [PubMed: 20536563]
47. Diggs LP, Hsueh EC. Utility of PD-L1 immunohistochemistry assays for predicting PD-1/PD-L1 inhibitor response. Biomark Res 2017;5:12 doi 10.1186/s40364-017-0093-8. [PubMed: 28331612]
48. Redman MW, Crowley JJ, Herbst RS, Hirsch FR, Gandara DR. Design of a phase III clinical trial with prospective biomarker validation: SWOG S0819. Clin Cancer Res 2012;18(15):4004–12 doi 10.1158/1078-0432.CCR-12-0167. [PubMed: 22592956]
49. Garon EB, Rizvi NA, Hui R, Leighl N, Balmanoukian AS, Eder JP, et al. Pembrolizumab for the treatment of non-small-cell lung cancer. N Engl J Med 2015;372(21):2018–28 doi 10.1056/NEJMoa1501824. [PubMed: 25891174]
50. Patel SP, Kurzrock R. PD-L1 Expression as a Predictive Biomarker in Cancer Immunotherapy. Mol Cancer Ther 2015;14(4):847–56 doi 10.1158/1535-7163.MCT-14-0983. [PubMed: 25695955]
51. Wang X, Wong K, Ouyang W, Rutz S. Targeting IL-10 Family Cytokines for the Treatment of Human Diseases. Cold Spring Harb Perspect Biol 2017 doi 10.1101/cshperspect.a028548.
52. Vahl JM, Friedrich J, Mittler S, Trump S, Heim L, Kachler K, et al. Interleukin-10-regulated tumour tolerance in non-small cell lung cancer. Br J Cancer 2017;117(11):1644–55 doi 10.1038/bjc.2017.336. [PubMed: 29016555]
53. Dennis KL, Blatner NR, Gounari F, Khazaie K. Current status of interleukin-10 and regulatory T-cells in cancer. Curr Opin Oncol 2013;25(6):637–45 doi 10.1097/CCO.0000000000000006. [PubMed: 24076584]

54. Trandem K, Zhao J, Fleming E, Perlman S. Highly activated cytotoxic CD8 T cells express protective IL-10 at the peak of coronavirus-induced encephalitis. J Immunol 2011;186(6):3642–52 doi 10.4049/jimmunol.1003292. [PubMed: 21317392]

55. Emmerich J, Mumm JB, Chan IH, LaFace D, Truong H, McClanahan T, et al. IL-10 directly activates and expands tumor-resident CD8(+) T cells without de novo infiltration from secondary lymphoid organs. Cancer Res 2012;72(14):3570–81 doi 10.1158/0008-5472.CAN-12-0721. [PubMed: 22581824]

56. Maybruck BT, Pfannenstiel LW, Diaz-Montero M, Gastman BR. Tumor-derived exosomes induce CD8(+) T cell suppressors. J Immunother Cancer 2017;5(1):65 doi 10.1186/s40425-017-0269-7. [PubMed: 28806909]

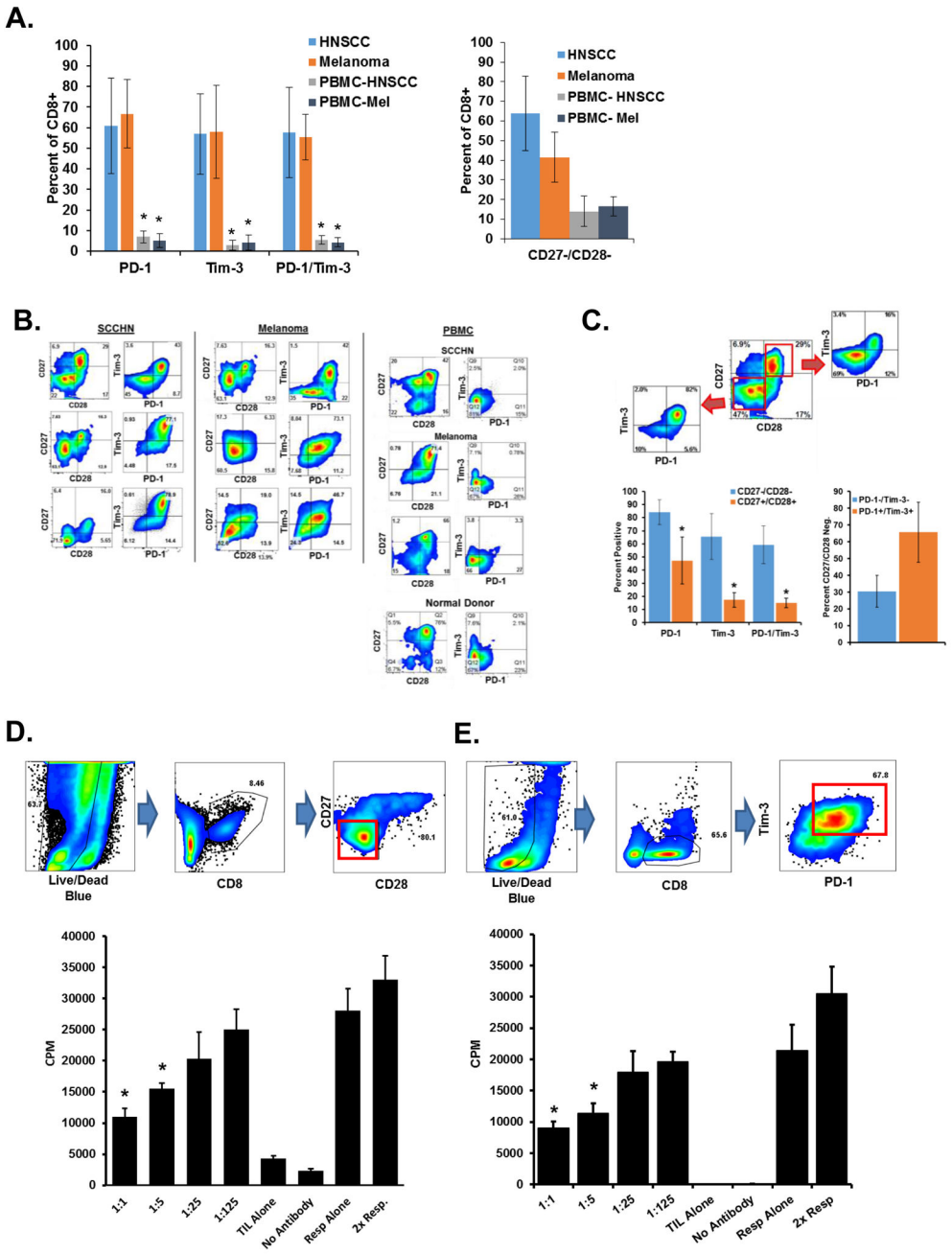

Figure 1. CD8$^+$ dysfunctional T cells in the human tumor microenvironment.

Tumor tissue was dissociated and indicated surface markers were stained. PBMCs were isolated from matching patient whole blood. **A.** Marker expression from eight SCCHN and seven melanoma patients. Error bars represent standard deviation. *$P < 0.05$ for expression of each marker (or group) as compared to the PBMC group using a student's T test. **B.** Representative flow cytometry stains of indicated patient SCCHN or melanoma tumors and PBMC. Plots are gated on CD3$^+$ and CD8$^+$ cells. **C.** Human tumor tissues from A. were gated on CD27 & CD28 expression and the PD-1$^+$ Tim-3$^+$ expression of these populations are represented (middle) with a representative dot plot (left) of a SCCHN patient used in

panel A. $CD27^{-}$ $CD28^{-}$ $CD8^{+}$ cells from the same patients were assessed for PD-1 and Tim-3 (right). Error bars indicate standard deviation. $*P < 0.05$ for the $CD27^{+}/CD28^{+}$ group vs. the $CD27^{-}/CD28^{-}$ group for each marker. **D.** $CD3^{+}$ $CD8^{+}$ PD-1^{+} Tim-3^{+} and $CD3^{+}$ $CD8^{+}$ $CD27^{-}$ $CD28^{-}$ cells were sorted from SCCHN tissue. Dot plots demonstrate gating to exclude tumor cells. Plots of ungated purified cells can be found in Supplementary Fig. S1A. Purified cells were then used in an *in vitro* suppression assays with autologous T cells. Proliferation was determined by ^{3}H-thymidine incorporation. Ratios indicate the number of suppressors to responders. Resp. = responders alone. Controls are using equivalent numbers of responder cells alone. **E.** $CD3^{+}$ $CD8^{+}$ PD-1^{+} Tim-3^{+} cells were sorted from SCCHN tumor tissue and used in *ex vivo* suppression assays. Ungated plots of sorted cells can be found in Supplementary Fig. S1B. Indicated data are representative of at least three independent experiments. Error bars represent SD of replicate wells for each condition. $*P < 0.05$ for the responders as compared to each experimental group using a student's t test.

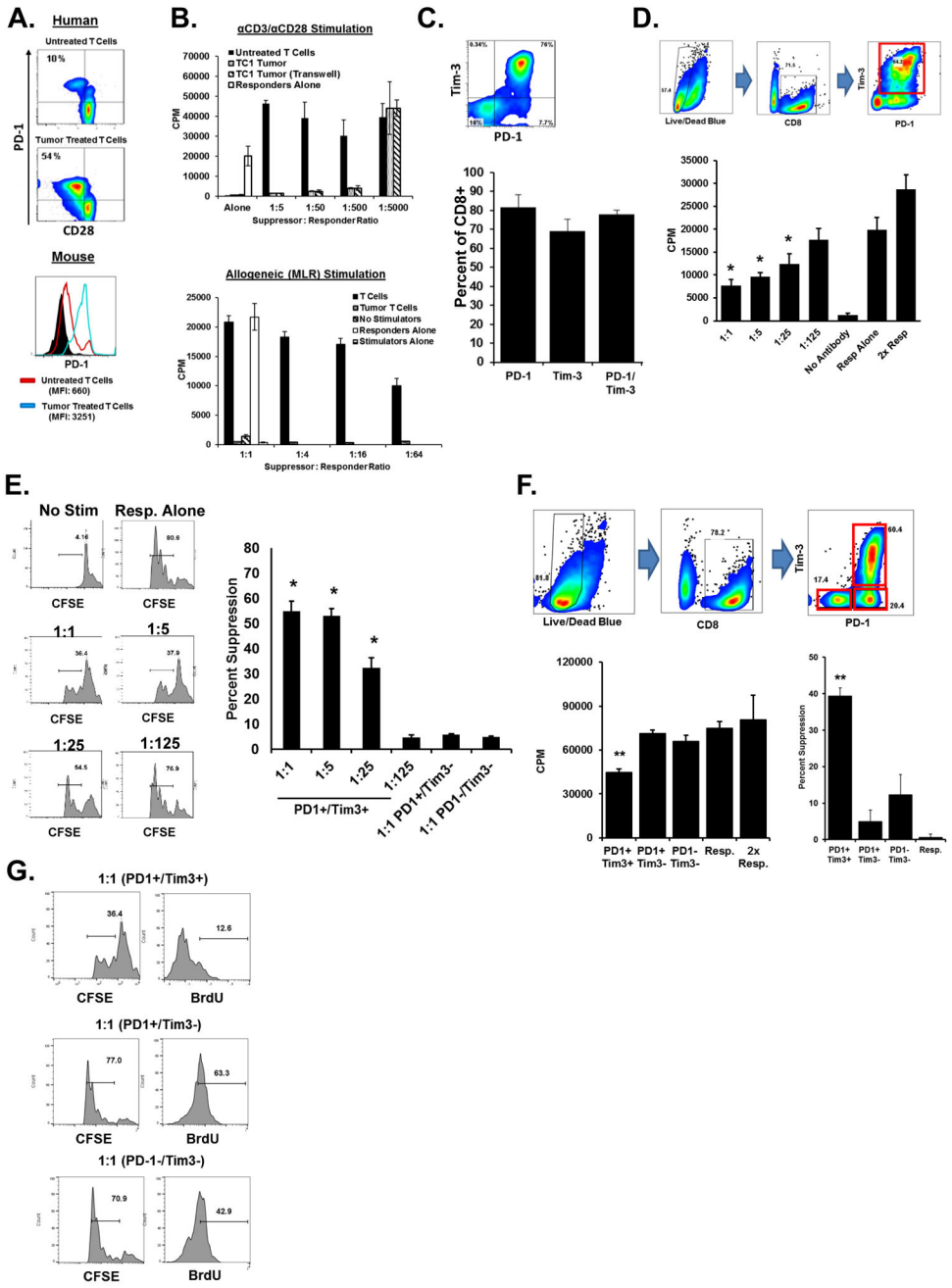

Figure 2. Development of an animal model of CD8$^+$ TIL suppression in SCCHN.

A. CD8$^+$ T cells purified from normal human donor PBMCs or from mouse splenocytes were incubated with equal numbers of TU167 (a human cell line) or TC-1 (a mouse cell line) for six hours. Cells were separated by transwell inserts. T cells were then washed and cultured for five days followed by staining for CD8, CD28, and PD-1 (for human cells) or CD8, Tim3, and PD-1 expression (for mouse cells). **B.** CD8$^+$ T cells were purified from mouse splenocytes and incubated with TC-1 tumor either directly or separated by a transwell insert for six hours. Cells were then separated and cultured for five days followed by use in *in vitro* suppression assays. Cells were stimulated with either anti-CD3/CD28 (top) or

allogeneic splenocytes (bottom). Proliferation was assessed by ^{3}H-thymidine incorporation. **C.** TC-1 tumors isolated from C57BL/6 mice were dissociated and stained for expression of CD3, CD8, and the indicated markers. Dot plots are gate on $CD3^{+}$ $CD8^{+}$ cells. Bar graphs represent at least 10 separate tumor samples. Error bars represent SD. **D.** $CD3^{+}$ $CD8^{+}$ cells were purified from dissociated TC-1 tumors using magnetic bead positive selection followed by use as suppressor cells in *in vitro* suppression assays. Ungated plots of sorted cells can be found in Supplementary Fig. S1C. Cells were incubated for 72h. **E.** In similar studys, responders were labeled with CFSE. Bar graph indicates percent suppression and incorporates three independent experiments. Histograms are representative. **F.** $CD3^{+}$ $CD8^{+}$ TILs from dissociated TC-1 tumors were sorted by PD-1 and Tim-3 expression into three groups as indicated. Plots of sorted cells can be found in Supplementary Fig. S1D. Purified cells were then used in *in vitro* suppression assays and proliferation was used to calculate percent suppression. **G.** Responders from F. were also labeled with CFSE and BrdU. Error bars represent standard deviation of replicate wells. Data is representative of at least three independent experiments. $^{**}P < 0.01$ for indicated population as compared to responders alone using a student's t test.

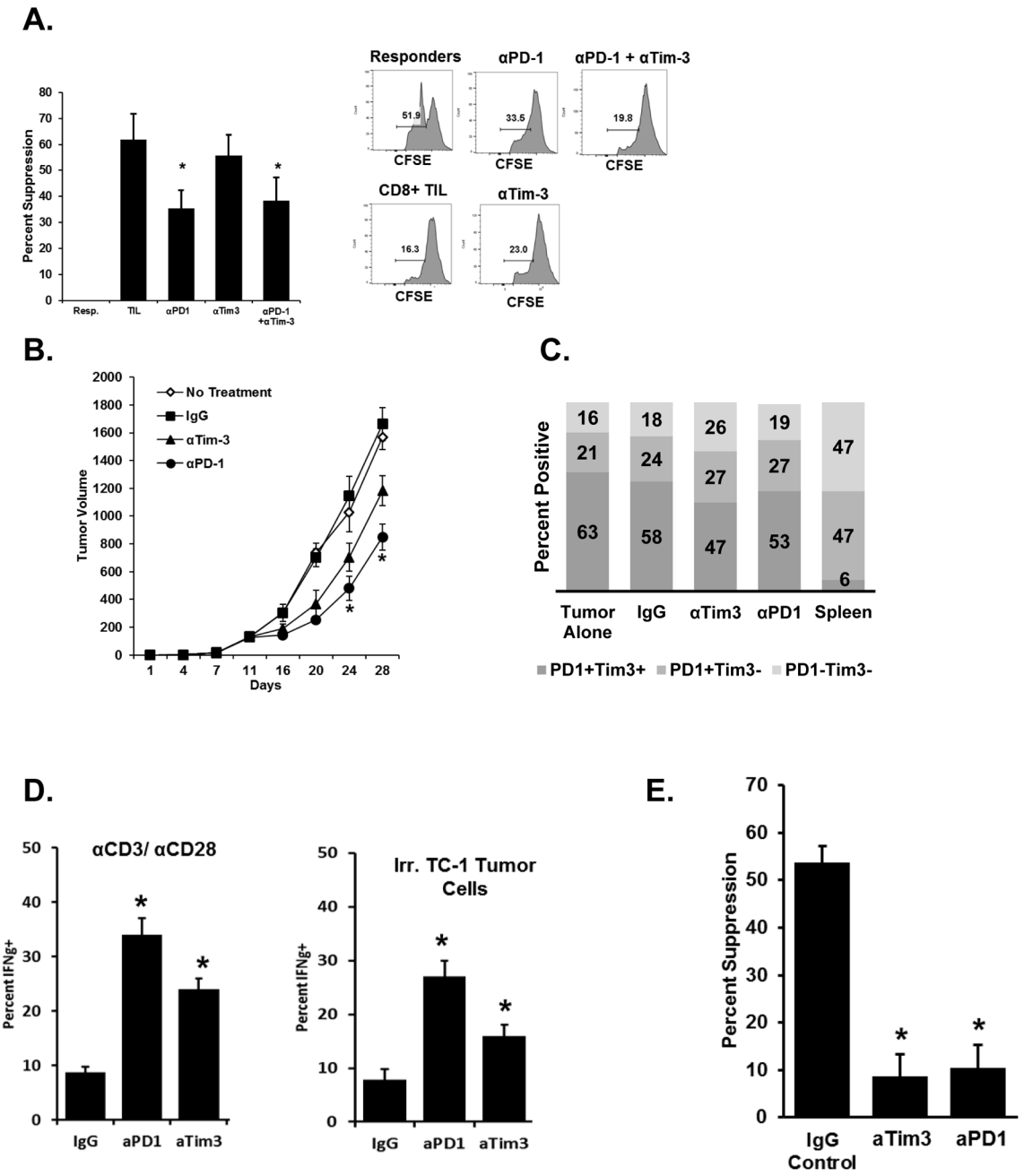

Figure 3. Blockade of checkpoint inhibitor proteins *in vivo* inhibits the suppressive function of CD8$^+$ TILs and enhances antitumor immunity.

A. PD-1$^+$ Tim-3$^+$ CD8$^+$ T cells were sorted from dissociated TC-1 tumors and used in *ex vivo* suppression assays. Antibodies against PD-1, Tim-3, or both were added to the cocultures. Proliferation was assessed via CFSE dilution or BrdU incorporation. CFSE dilution was used to determine percent suppression. **B.** TC-1 tumor cells were implanted s.c. into mice (n=10 per group). Five days later treatment groups received 100μg of the indicated antibodies i.p. Injections were repeated every three days thereafter. *P<0.05 for the combination group vs. others at the indicated time points using ANOVA analysis. **C.** At the

conclusion of the study, expression of PD-1 and Tim-3 on $CD8^+$ TILs was assessed by flow cytometry ($n = 10$ tumors per group). For comparison, splenocytes from non-tumor-bearing mice were stained with a similar panel. **D.** $CD8^+$ TILs were purified from tumor digests using magnetic beads and stimulated *in vitro* as indicated for 12 hours (N = 10 per group, representative of three independent studies). Cells were then stained for interferon-γ expression. **E.** $CD8^+$ $PD\text{-}1^+$ $Tim\text{-}3^+$ TILs were sorted from tumors as and used in *in vitro* suppression assays. Data are reported as the percent suppression as compared to responders alone. Error bars indicate standard deviation. $*P<0.05$ for the indicated treatment groups vs IgG control using a Student *t* test.

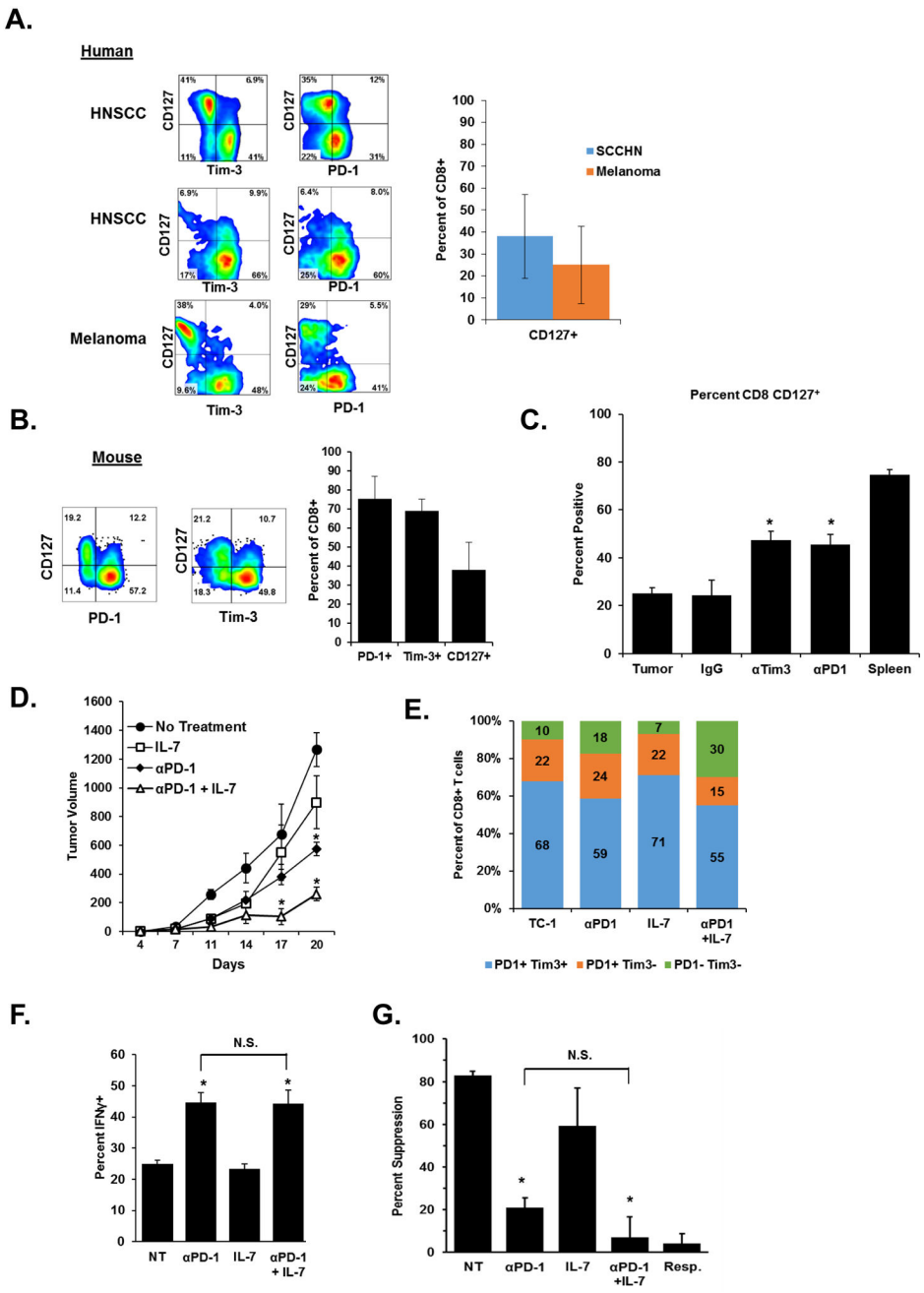

Figure 4. Treatment with IL7 synergizes with anti-PD-1 blockade to enhance antitumor immune responses.

A. Tumor tissue from two HNSCC and one melanoma patient were stained for expression of CD127, PD-1, and Tim-3 on $CD3^+$ $CD8^+$ T cells. Graphs indicate the percentage of CD127 on tumor-resident T cells in twelve HNSCC and melanoma patients or normal donor PBMC. **B.** Expression of CD127 on $CD8^+$ TILs from TC-1 tumors. Graphs indicate the percentage of PD-1, Tim-3, and $CD127^+$ cells in six tumors. **C.** Expression of CD127 was assessed on $CD8^+$ TILs from tumors treated with the indicated antibodies or combinations as used in Fig. 3. Similar staining of splenocyte $CD8^+$ T cells is included as a comparison. **D.** TC-1

tumor cells were implanted s.c. into mice (n=10 per group). Five days later, treatment groups received 100μg of anti-PD-1 i.p. Injections were repeated every three days thereafter. IL7 treated mice received 10μg rhIL7 i.p. every 24 hours for seven days. **P* <0.05 for the combination group vs. others at the indicated time points. **E.** At the conclusion of the study, PD-1 and Tim-3 expression on $CD8^+$ T cells was determined (*n* = 8 mice per group). **F.** $CD8^+$ TILs were purified from tumor digests using magnetic beads and stimulated *in vitro* for 12 hours followed by staining for IFNγ expression (N = 8 mice per group, representative of three independent experiments). "NT" indicates the no-treatment control group. **G.** $CD3^+$ $CD8^+$ $PD\text{-}1^+$ $Tim\text{-}3^+$ TILs were sorted and used in *in vitro* suppression assays. Data are reported as percent suppression as compared to responders alone. Error bars indicate standard deviation. **P* <0.05 for the IgG treated group vs. other treatments using a student's t test.

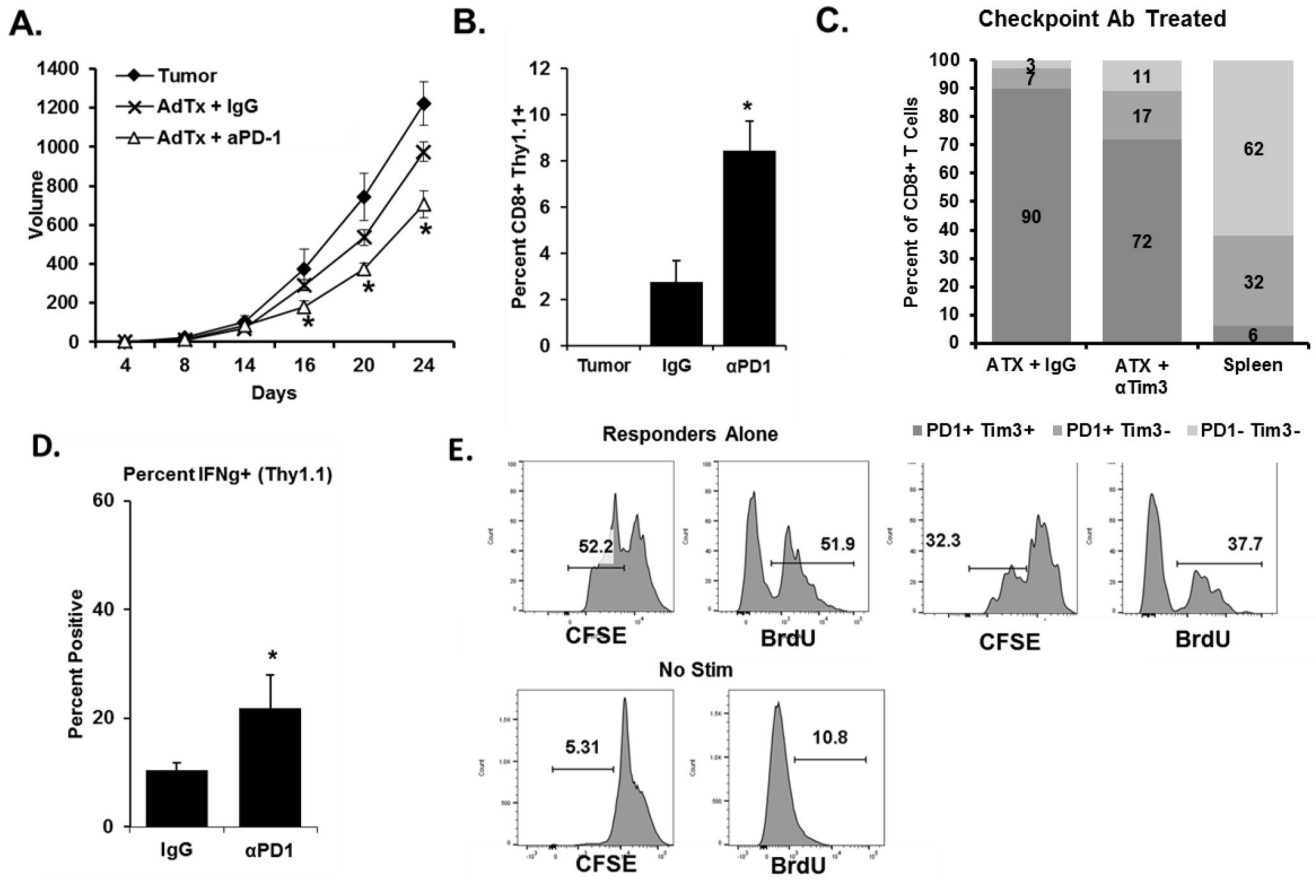

Figure 5. Checkpoint inhibitor blockade enhances antitumor treatment by CD8$^+$ adoptive T-cell transfer.

A. TC-1 tumors were implanted into mice on day 0 followed by adoptive transfer of purified E7 TCRβ T cells and 100μg of anti-PD-1 or control antibodies i.p. on day 5 (n=10 per group). Antibody treatment was repeated every three days. Tumor growth (n = 8 per group) was measured at the indicated time points. *P < 0.05 for the combination treatment vs other groups using ANOVA at the indicated time points. **B**. At the conclusion of the study, the percentage of adoptively transferred cells in the total TIL population was determined. Error bars indicate standard deviation. **C.** Concurrently, TILs were stained for PD-1 and Tim-3 expression. Similar staining of splenocyte CD8$^+$ T cells from a non-tumor-bearing mouse is also displayed for comparison. **D.** CD8$^+$ TILs were then restimulated *in vitro* and interferon-γ production was assessed. Error bars indicate standard deviation, *P < 0.05 for the anti-PD-1 treated group vs control. **E.** PD-1$^+$ Tim-3$^+$ CD8$^+$ Thy1.1$^+$ TILs pooled from 8 mice were used in *ex vivo* suppression assays using CFSE dilution and BrdU incorporation as a readout of proliferation. Histograms are representative of three experiments.

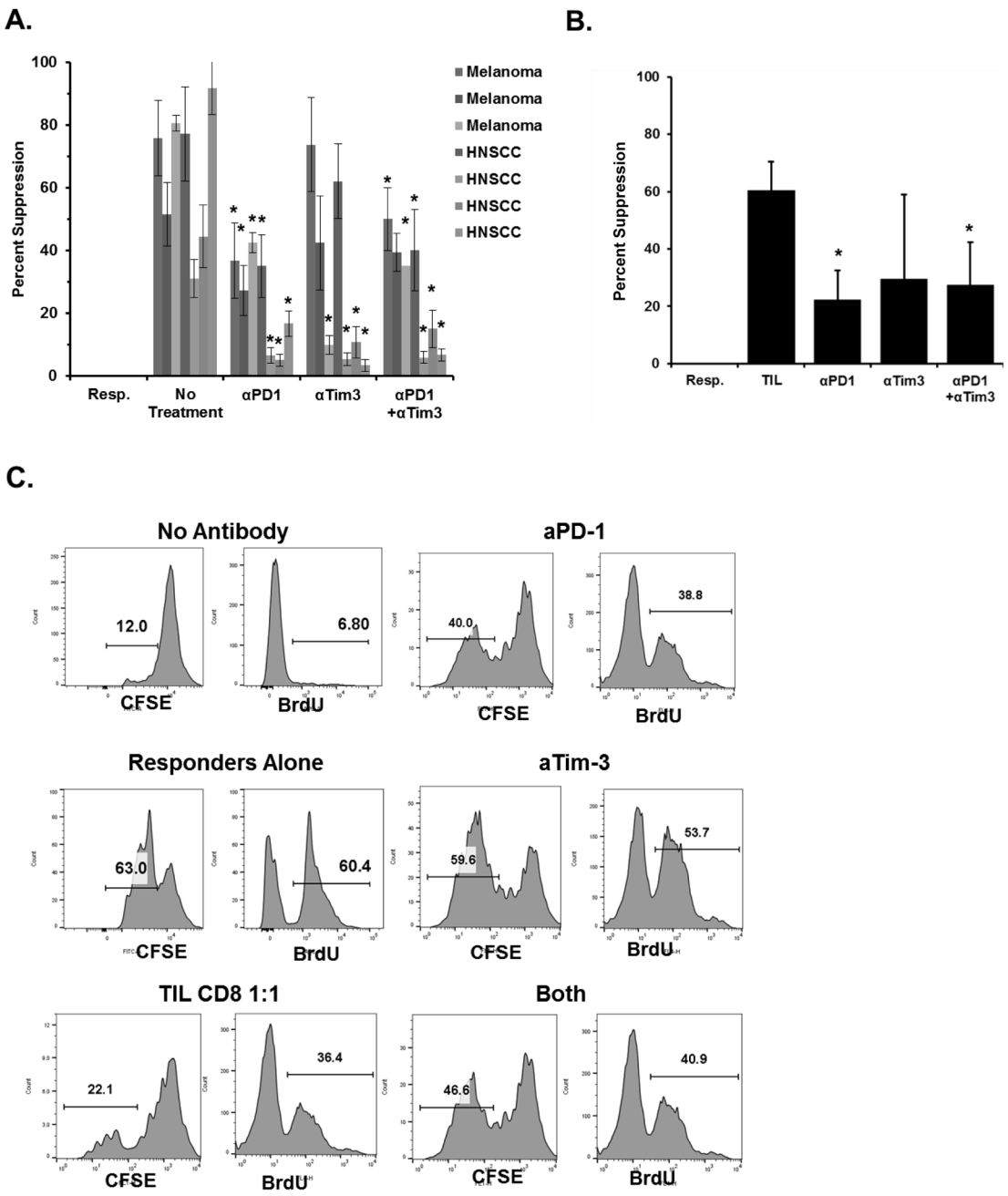

Figure 6. Checkpoint inhibitor blockade *ex vivo* reduces the suppressive function of CD8$^+$ TIL.

A. Melanoma and SCCHN tumors from human patients were dissociated and CD3$^+$ CD8$^+$ PD-1$^+$ Tim-3$^+$ TILs were purified by sorting and then used in *in vitro* suppression assays with autologous PBMC T cells. Antibodies against the indicated checkpoint inhibitor proteins were added during the co-incubation. *P <0.05 for the indicated groups vs. the no-treatment group from the same patient using a student's t test. **B.** Percent suppression of each treatment group as compared to responders alone and is cumulative of all samples in A. Error bars indicate the standard deviation of replicate wells. **C.** CD3$^+$ CD8$^+$ PD-1$^+$ Tim-3$^+$ TILs from a human melanoma patient were purified by sorting and used *in vitro* suppression

assays with purified T cells from PBMC's from the same patient as described in A using CFSE dilution or BrdU incorporation. Histograms are representative of three replicates.

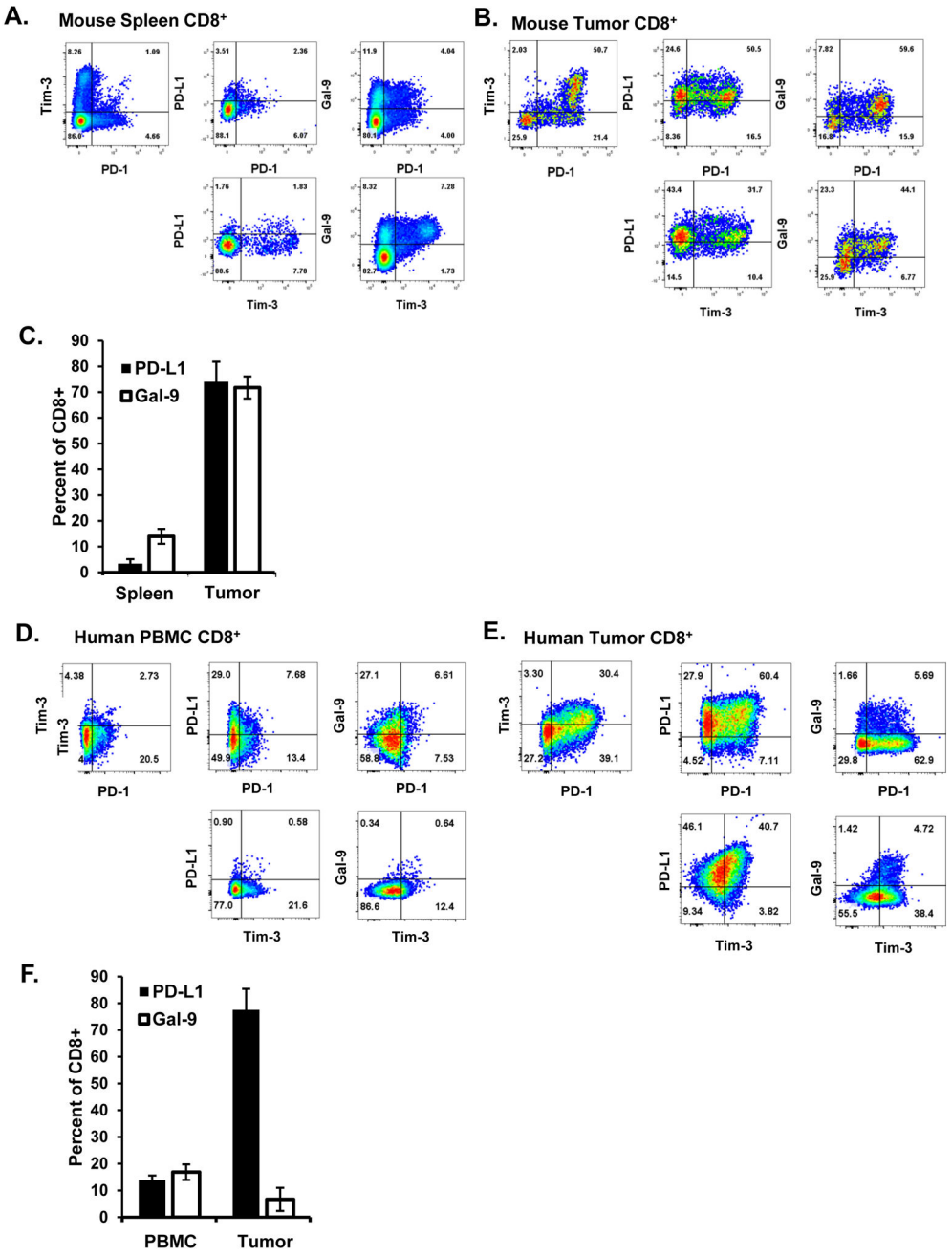

Figure 7. PD-1 and Tim-3 ligand expression in the mouse and human tumor microenvironment.

Mouse tissue from (**A**) spleen and (**B**) eight TC-1 tumors was stained for the indicated markers. (**C**) Cumulative percentages of PD-L1$^+$ and Gal-9$^+$ cells . Error bars represent standard deviation. Human (**D**) PBMCs from three normal donors or from (**E**) five human melanoma specimans were similarly stained. **E**, Cumulative percent-positive cells for PD-L1 and Gal-9. Error bars represent standard deviation.

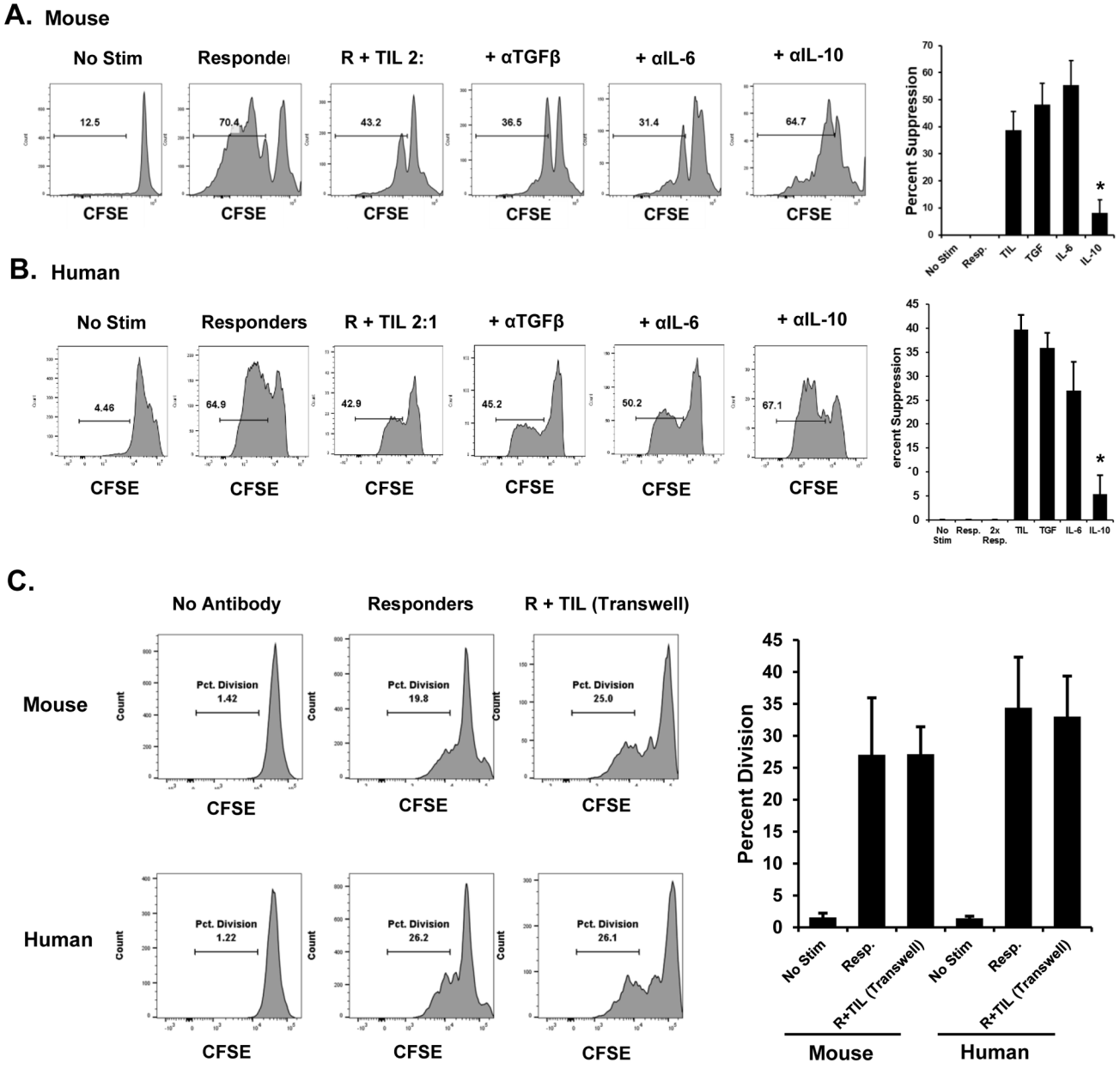

Figure 8. Mechanism of suppression by CD8$^+$ TIL.

A,Mouse CD8$^+$ PD-1$^+$ Tim-3$^+$ TILs were FACS-sorted from dissociated TC-1 tumors and used in *in vitro* suppression assays with the indicated blocking antibodies. Responder cells were labeled with CFSE. At the conclusion of the experiment, cells were analyzed by flow cytometry. Plots are representative of at least three replicates per sample. Data from all replicates were used to calculate percent suppression. **B**, Similar studies were conducted using PD-1$^+$ Tim-3$^+$ CD8$^+$ T cells FACS-sorted from human patient specimens ($n = 4$) with autologous T cells as responders. Error bars represent standard deviation between the replicate samples. *$P < 0.05$ for the anti-IL10 –treated group as compared to the TIL alone group. **C**, PD-1$^+$ Tim-3$^+$ CD8$^+$ T cells were sorted from TC-1 tumors or human melanoma tumors and used in *in vitro* suppression assays with autologous responder T cells.

Suppressors were physically separated from responder cells via transwell inserts. Responders were seeded onto the anti-CD3/CD28 coated lower plate. Proliferation was assessed by CFSE dilution. Plots are representative of three independent experiments which were used to cumulatively display percent division of each group in the bar graph. Error bars indicate standard deviation.